Heterogeneous Electron Transfer Kinetics at the Ionic Liquid/Metal Interface Studied Using Cyclic Voltammetry and Scanning Electrochemical Microscopy

ARTICLE *in* THE JOURNAL OF PHYSICAL CHEMISTRY B · OCTOBER 2008

Impact Factor: 3.3 · DOI: 10.1021/jp8024717 · Source: PubMed

Heterogeneous Electron Transfer Kinetics at the Ionic Liquid/Metal Interface Studied Using Cyclic Voltammetry and Scanning Electrochemical Microscopy

Alasdair W. Taylor, Fulian Qiu, Jingping Hu, Peter Licence,* and Darren A. Walsh*

School of Chemistry, The University of Nottingham, Nottingham NG7 2RD, U.K.

Received: March 20, 2008

The electrochemical behavior of a redox-active, ferrocene-modified ionic liquid (1-ferrocenylmethyl-3-methylimidazolium bis(trifluoromethylsulfonyl)imide) in acetonitrile and in an ionic liquid electrolyte (1-ethyl-3-methylimidazolium bis(trifluoromethylsulfonyl)imide) is reported. Reversible electrochemical behavior was observed in each electrolyte with responses typical of those for unmodified ferrocene observed in each medium. In the ionic liquid electrolyte, the diffusion coefficient of the redox-active ionic liquid increased by a factor of 5 upon increasing the temperature from 27 to 90 °C. The kinetics of electron transfer across the ionic liquid/electrode interface were studied using cyclic voltammetry, and the standard heterogeneous electron transfer rate constant, k^0 was determined to be 4.25×10^{-3} cm s^{-1}. Scanning electrochemical microscopy was then also used to probe the heterogeneous kinetics at the interface between the ionic liquid and the solid electrode and conventional kinetic SECM theory was used to determine k^0. The k^0 value obtained using SECM was higher than that determined using cyclic voltammetry. These results indicate that SECM is a very useful technique for studying electron transfer dynamics in ionic liquids.

Introduction

Room temperature ionic liquids (RTILs) have received increasing attention in recent years due to their many unique physical and chemical properties.[1−3] These include negligible vapor pressure, high chemical and thermal stability, high conductivity, and their ability to dissolve a wide range of organic and inorganic compounds. As a result, RTILs have been employed in such diverse areas as organic synthesis,[4,5] chemical extraction,[6,7] and enzymatic catalysis.[8,9] As RTILs can act as both solvent and electrolyte, they are also being used in an increasing number of electrochemical applications, including supercapacitors,[10,11] batteries,[12,13] dye-sensitized solar cells,[14,15] and electrodeposition.[16,17] First-generation haloaluminate RTILs initially received much attention for electrochemical applications. However, because of substantial air- and moisture-sensitivity, wider applications of haloaluminate RTILs have been limited. Second-generation RTILs, containing anions such as tetrafluoroborate, $[BF_4]^-$, hexafluorophosphate, $[PF_6]^-$, and bis(trifluoromethylsulfonyl)imide, $[NTf_2]^-$, were subsequently developed, which showed better air and water stability.[18] Of these RTILs, those containing the $[NTf_2]^-$ anion showed the best stability as they do not form HF when in contact with water.[19]

Electrochemical investigations of the mass and charge-transfer kinetics of a variety of redox species have been studied using second-generation RTILs.[20−22] However, some practical challenges remain when performing electrochemical measurements in RTILs, including selecting a suitable reference electrode.[23−25] Efficient removal of water can also be extremely important as the electrochemical potential window of many RTILs narrows as the water content increases.[26] Adventitious water can also have a dramatic effect on viscosity. For example, 2% water in 1-butyl-3-methylimidazolium tetrafluoroborate decreases the viscosity by as much as 50%.[4] The most commonly used method for water removal from RTILs is heating under vacuum but, because of their hygroscopic nature, ionic liquids can rapidly reabsorb atmospheric water. Despite this, ionic liquids are extremely promising for electroanalytical applications due to their broad potential windows, high conductivities, and high thermal stabilities.[27−29]

Scanning electrochemical microscopy (SECM) has been shown to be an extremely useful tool for studying electrochemical phenomena at a range of substrates and interfaces and has been used recently to probe electron transfer at the RTIL/water interface.[30,31] The feedback mode of SECM, where the steady-state current, $i_{T,\infty}$ of an ultramicroelectrode (UME) tip is perturbed by positioning it close to a substrate electrode, is especially useful for studying heterogeneous electron transfer kinetics.[32] However, no studies have been reported to date that successfully exploited the power of SECM to perform kinetic measurements in single-phase ionic liquids. This is usually due to difficulties encountered when attempting to record steady-state voltammograms at the SECM tip. SECM theory, which is used for kinetic analysis, requires the establishment of a steady-state current at the SECM tip. The feasibility of using SECM in single-phase ionic liquids has recently been examined, and it was concluded that long experimental timescales (slow voltammetric scan rates) and very small SECM tips were essential to record good-quality steady-state voltammograms.[33] It has also been proposed that inequalities of the diffusion coefficients of the reduced and oxidized species can complicate SECM measurements.[34]

In this contribution, we describe the voltammetric behavior and heterogeneous kinetics of a new class of redox-active ionic liquid. Ferrocene-modified imidazolium salts were introduced a number of years ago and have been used as synthetic intermediaries and ion receptors.[35−37] However, few reports exist that describe the electrochemical properties of this important class of electroactive materials. Recently, Murray and co-workers demonstrated the voltammetric behavior of undiluted

* To whom correspondence should be addressed: E-mail: darren.walsh@nottingham.ac.uk (D.A.W.), peter.licence@nottingham.ac.uk (P.L.). Tel: +44 115 951 3437or +44 115 846 6176. Fax: +44 115 951 3562.

10.1021/jp8024717 CCC: $40.75
Published on Web 09/30/2008

SCHEME 1: Structure of (A) [FcC$_1$MIm][NTf$_2$] and (B) [C$_2$MIm][NTf$_2$]

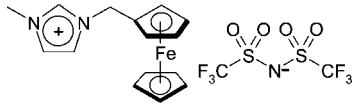

A

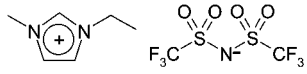

B

1-ferrocenylmethyl-3-methylimidazolium bis (trifluoromethylsulfonyl)imide, [FcC$_1$MIm][NTf$_2$], as well as when diluted using dichloromethane.[38] However, the mass transport properties and heterogeneous electron transfer kinetics of these materials remain unknown. Here, we describe the electrochemical behavior of [FcC$_1$MIm][NTf$_2$], dissolved in a second, electrochemically inactive ionic liquid (1-ethyl-3-methylimidazolium bis(trifluoromethyl-sulfonyl)imide), [C$_2$MIm][NTf$_2$] (Scheme 1). Remarkably ideal voltammetric behavior was observed in this system, which allowed us to explore the mass-transport dynamics of the redox-active RTIL. Given the extremely high thermal stability of these RTILs, it was also possible to examine the effect of temperature on the mass-transport dynamics of the system using variable-temperature voltammetry.

We also describe the use of SECM to probe the kinetics of heterogeneous electron across the RTIL/electrode interface. Despite the reduced diffusion coefficient of [FcC$_1$MIm][NTf$_2$], high-quality steady-state voltammograms were observed at Pt SECM tips. By positioning an SECM tip sufficiently close to a platinum substrate electrode (tip-substrate separation <1 μm), it was possible to probe the heterogeneous electron transfer kinetics at the SECM tip. Conventional SECM theory was then successfully used to estimate the heterogeneous electron transfer rate constant, k^0, which was compared with that determined using cyclic voltammetry. Thus, these results show, for the first time, that kinetic measurements may be performed in ionic liquids using the SECM, and we suggest that solvation of the analyte may be the crucial factor in such measurements.

Experimental Section

Reagents and Apparatus. All chemicals were obtained from Sigma-Aldrich or Alfa Aesar and were used as received except for 1-methylimidazole, which was distilled over calcium hydride prior to use. Lithium bis(trifluoromethylsulfonyl)imide was obtained from 3M and used as received. HPLC-grade acetonitrile (Aldrich, 99.9% purity) was used for electrochemical experiments. ^{1}H, ^{13}C, and ^{19}F NMR spectra were recorded on a Bruker DPX-300 MHz spectrometer. Cyclic voltammetry was performed using a Model 760 C potentiostat from CH Instruments (Austin, Texas, USA) or an Autolab 30 potentiostat (Eco Chemie B.V., The Netherlands). SECM measurements were performed using a Model 910B SECM from CH Instruments.

Electrochemical Measurements. Electrochemical measurements in RTILs were performed using a standard three-electrode cell, consisting of a platinum wire counter electrode and an Ag|Ag$^+$ reference electrode. The Ag|Ag$^+$ reference electrode was fabricated by inserting a clean silver wire into a solution (10 mM) of silver trifluoromethanesulfonate in [C$_2$MIm][NTf$_2$] using a similar procedure to that described previously.[39] The stability of this reference electrode was measured by recording cyclic voltammograms (CVs) at a platinum electrode in a solution of [FcC$_1$MIm][NTf$_2$] in [C$_2$MIm][NTf$_2$] and recording the half-wave potential of the redox couple relative to the reference electrode. The potential was stable to within a few millivolts for up to four weeks. CVs in acetonitrile were recorded using a silver-wire quasi-reference electrode (AgQRE). A 0.58 mm or 0.25 mm diameter platinum disk electrode was used as the working electrode for general electrochemical measurements. Prior to use, the working electrode was polished using an aqueous suspension of 0.05 μm alumina (Buehler, Lake Bluff, Illinois), sonicated in an ultrasonic bath in a small amount of water and rinsed thoroughly with deionized water. Variable-temperature cyclic voltammetry was performed by immersing the entire three-electrode cell in a temperature-controlled oil bath. Kinetic parameters were obtained from experimental CVs by fitting them to simulated voltammograms generated according to the Butler−Volmer formulation of electrode kinetics using a finite difference method simulation ran using Fortran. Before fitting the experimental CVs to the theoretical response, a background subtraction was performed by recording a CV in blank electrolyte and subtracting it digitally from the experimental CV.

SECM tips were prepared by heat-sealing a platinum wire (25 μm diameter, Goodfellow, UK) into a quartz capillary and then pulling to a fine point using a laser-micropipet puller (Model P2000, Sutter Instrument Co., Novato, California) using a similar procedure to that reported previously.[40] The platinum metal surface was exposed and bevelled using a commercially available microelectrode beveller (Model BV-10, Sutter Instrument Co., Novato, California) producing a sharpened SECM tip. SECM tips were then examined using optical microscopy. The radius of the tip used in this study was approximately 1.5 μm with an *RG* value ($= r_g/a$, where r_g is the radius of the insulating glass sheath and a is the radius of the platinum wire) of approximately 2. The radius of the SECM tip was confirmed using cyclic voltammetry and SECM feedback approach curve experiments (described later). The tip surface was gently polished using the microelectrode beveller between measurements.

Synthesis of Ionic Liquids. [C$_2$MIm][NTf$_2$] was synthesized from 1-ethyl-3-methylimidazolium ethylsulfate as described previously.[19,28] [FcC$_1$MIm][NTf$_2$] was synthesized from *N*,*N*-dimethylaminomethylferrocene methiodide as follows:

Synthesis of 1-Ferrocenylmethylimidazole. A mixture of *N*,*N*-dimethylaminomethylferrocene methiodide (20 g, 0.05 mol) and imidazole (8.17 g, 0.12 mol) was refluxed in dimethyl formamide (100 mL) for 2 h. The resulting red-brown solution was hydrolyzed with 100 mL water and the product was then extracted into diethyl ether (5 × 75 mL). The combined organic phase was washed with water (3 × 150 mL) and dried over $MgSO_4$. The solvent was removed by rotary evaporation to give light-orange crystals (7.16 g, 55%).

^{1}H NMR, δ_H (300 MHz, DMSO-d_6), 7.65 (1H, s, NCHN), 7.15 (1H, s, CCHN), 6.83 (1H, s, NCHC), 4.90 (2H, s NCH_2Fc), 4.31 (2H, t, CCH), 4.18 (5H, s, C_5H_5), 4.17 (2H, dd, CHCH).

^{13}C NMR δ_c (75 MHz, DMSO-d_6), 136.76, 128.10, 119.20, 84.20, 68.49, 68.43, 68.07, 45.34.

Synthesis of 1-Ferrocenylmethyl-3-methylimidazolium Iodide. Methyl iodide (3.1 g, 22 mmol) was added dropwise to a stirred solution of 1-ferrocenylmethylimidazole (2.7 g, 10.6 mmol) in ethyl acetate (10 mL). The solution was then heated at 40 °C for 2 h. The orange product was obtained by vacuum

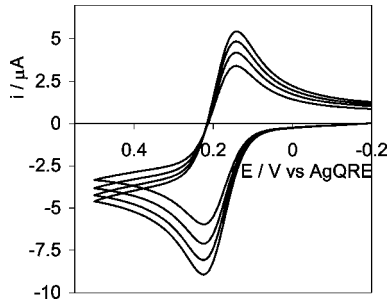

Figure 1. Cyclic voltammograms obtained in 5 mM $[FcC_1MIm][NTf_2]$ in acetonitrile containing 0.1 M $[Bu_4N][BF_4]$ as supporting electrolyte at 25 °C. The scan rates were (from top to bottom) 0.5, 0.4, 0.3, and 0.2 V s^{-1}, and the potential was scanned between −0.2 and 0.5 V vs Ag QRE. The initial potential was −0.2 V in each case.

filtration and washed with ethyl acetate (3 × 5 mL). Residual solvent was removed in vacuo to yield 3.5 g (83%) of an orange powder.

^{1}H NMR, δ_H (300 MHz, DMSO-d_6), 9.10 (1H, s, NCHN), 7.76 (1H, t, CHCHN), 7.66 (1H, s, NCHCH), 5.18 (2H, s, NCH_2Fc), 4.45 (2H, t, FcH), 4.23 (7H, s, FcH), 3.83 (3H, t, NCH_3).

^{13}C NMR δ_c (75 MHz, DMSO-d_6), 136.70, 124.45, 122.87, 81.83, 69.86, 69.73, 69.60, 49.16, 36.74.

Synthesis of 1-Ferrocenylmethyl-3-methylimidazolium Bis-(trifluoromethylsulfonyl)imide. Lithium bis(trifluoromethylsulfonyl)imide (0.87 g, 3 mmol) in water (5 mL) was added dropwise to a solution of 1-ferrocenylmethyl-3-methylimidazolium iodide (1 g, 2.5 mmol) in water (10 mL). The reaction was then stirred at 40 °C for 18 h. The water was decanted from the biphasic mixture and the ionic liquid phase was dissolved in dichloromethane (10 mL). The organic phase was then washed with water (3 × 5 mL). The solvent was removed in vacuo yielding a red−brown liquid, which subsequently crystallized (1.23 g, 90%).

^{1}H NMR, δ_H (300 MHz, DMSO-d_6), 9.04 (1H, s, NCHN), 7.71 (1H, t, CHCHN), 7.63 (1H, t, NCHCH), 5.15 (2H, s, NCH_2), 4.43 (2H, t, FcH), 4.24 (7H, t, FcH), 3.81 (3H, s, NCH_3).

^{13}C NMR δ_c (75 MHz, DMSO-d_6), 136.72, 124.45, 122.85, 81.75, 69.79, 69.74, 69.57, 49.16, 36.61.

^{19}F NMR δ_F (282 MHz, DMSO-d_6), −79.71.

Results and Discussion

Electrochemical Behavior of $[FcC_1MIm][NTf_2]$ in Acetonitrile. Figure 1 shows typical CVs recorded at various scan rates in 5 mM $[FcC_1MIm][NTf_2]$ dissolved in acetonitrile containing 0.1 M $[Bu_4N][BF_4]$ as supporting electrolyte. At each scan rate, v, the ratio of the anodic peak current, $i_{p,a}$, to the cathodic peak current, $i_{p,c}$, was close to 1, the anodic and cathodic peak potentials, $E_{p,a}$ and $E_{p,c}$, were independent of v and i_p increased with $v^{1/2}$. These observations are consistent with those expected for a freely diffusing species in solution.[41] Moreover, these observations are similar to those observed for solutions of ferrocene in acetonitrile.[42] The diffusion coefficient of $[FcC_1MIm][NTf_2]$, calculated from the gradient of a linear plot of i_p vs $v^{1/2}$, was 1.22 (±0.05) × 10^{-5} cm^2 s^{-1}. This value is similar to that reported for ferrocene in acetonitrile,[43] indicating that modification of ferrocene with the imidazolium moiety did not affect its rate of diffusion in acetonitrile to any significant extent.

Electrochemical Behavior of $[FcC_1MIm][NTf_2]$ in $[C_2MIm][NTf_2]$. Part A of Figure 2 shows typical cyclic voltammograms recorded using 3 mM $[FcC_1MIm][NTf_2]$ in $[C_2MIm][NTf_2]$ at

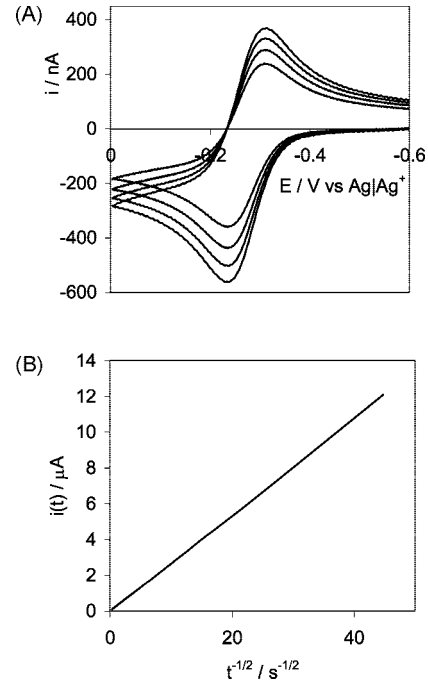

Figure 2. (A) Cyclic voltammograms obtained using a 3 mM solution of $[FcC_1MIm][NTf_2]$ in $[C_2MIm][NTf_2]$ at 27 °C. The scan rates were (from top to bottom) 0.5, 0.4, 0.3, and 0.2 V s^{-1} and the potential was scanned between −0.6 and 0.0 V vs $Ag|Ag^+$. The initial potential was −0.6 V in each case. (B) Chronoamperometric $i(t)$ versus t (Cottrell) plot obtained at a nominally 0.25 mm radius platinum disk electrode in 5.08 mM $[FcC_1MIm][NTf_2]$ in $[C_2MIm][NTf_2]$. The potential was stepped from −0.4 to 0.0 V vs $Ag|Ag^+$ to drive the oxidation of the ferrocene moiety at a diffusion-controlled rate.

various scan rates. The voltammograms are similar in appearance to those observed using acetonitrile as solvent. The ratio of $i_{p,a}$ to $i_{p,c}$ was close to 1 and i_p was proportional to $v^{1/2}$, which indicate that mass transfer of $[FcC_1MIm][NTf_2]$ to the electrode surface was also diffusion-controlled in the RTIL electrolyte. The formal potential, $E°'$, of the $[FcC_1MIm]^+/[FcC_1MIm]^{2+}$ redox couple was −0.263 V versus $Ag|Ag^+$. The diffusion coefficient of $[FcC_1MIm][NTf_2]$, calculated from the gradient of linear plots of i_p vs $v^{1/2}$, was 1.07 (±0.05) × 10^{-7} cm^2 s^{-1}, which is 2 orders of magnitude smaller than that observed in acetonitrile. Chronoamperometry was also used to calculate the diffusion coefficient of $[FcC_1MIm][NTf_2]$ and a representative $i(t)$ versus $t^{-1/2}$ (Cottrell) plot is shown in part B of Figure 2. From the slope of the linear Cottrell plots, the diffusion coefficient of $[FcC_1MIm][NTf_2]$ was calculated as 1.06 × 10^{-7} cm^2 s^{-1}, which agreed closely with that determined using cyclic voltammetry. The smaller diffusion coefficient in the RTIL compared to a traditional organic solvent has been reported for various other redox species, including ferrocene and is most likely due the high viscosity of the RTIL solvent.[44,33]

Effect of Temperature on Diffusion Coefficient. Part A of Figure 3 shows typical voltammograms recorded using a solution of $[FcC_1MIm][NTf_2]$ in $[C_2MIm][NTf_2]$ at 27, 55, 75, and 90 °C. Clearly, $E°'$ did not vary with temperature and the ratios of $i_{p,a}$ to $i_{p,c}$ remained close to 1 at all temperatures. Part B of Figure 3 shows the dependence of the anodic and cathodic peak currents on $v^{1/2}$ at various temperatures, which illustrates that plots of i_p versus $v^{1/2}$ were linear at all temperatures. The increasing gradients of these plots with increasing temperature indicates an increase in the rate of diffusion of the electroactive species at higher temperatures. Table 1 shows the diffusion coefficients of $[FcC_1MIm]^+$ and $[FcC_1MIm]^{2+}$ at each temper-

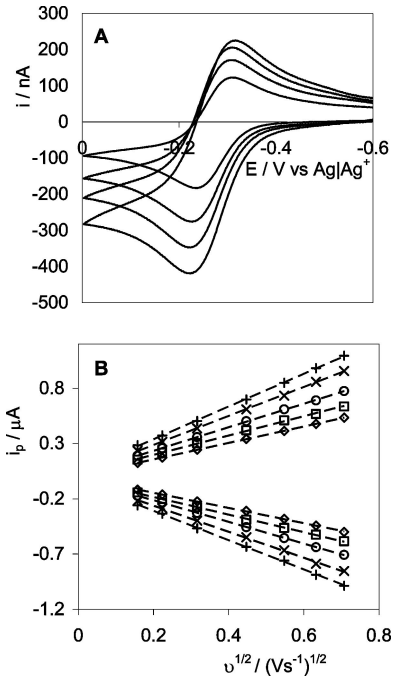

Figure 3. (A) Cyclic voltammograms obtained using a 5 mM solution of $[FcC_1MIm][NTf_2]$ in $[C_2MIm][NTf_2]$ at (from top to bottom) 90, 75, 55, and 27 °C. The voltammetric scan rate was 50 mV s^{-1} in each case and the potential was scanned between −0.6 and 0.0 V vs $Ag|Ag^+$. The initial potential was −0.6 in each case. (B) Plots of i_p versus $\upsilon^{1/2}$ for 5 mM $[FcC_1MIm][NTf_2]$ in $[C_2MIm][NTf_2]$ at temperatures of 27 °C (◇), 40 °C (□), 55 °C (○), 75 °C (×), and 90 °C (+).

TABLE 1: Diffusion Coefficients of $[FcC_1MIm]^+$ and $[FcC_1MIm]^{2+}$ at Various Temperatures

T/°C	$D_{[FcC1MIm]^+}$/cm^2 s^{-1}	$D_{[FcC1MIm]^{2+}}$/cm^2 s^{-1}
27	1.07×10^{-7}	0.914×10^{-7}
40	1.57×10^{-7}	1.33×10^{-7}
55	2.40×10^{-7}	2.01×10^{-7}
75	3.84×10^{-7}	3.14×10^{-7}
90	5.29×10^{-7}	4.32×10^{-7}

ature. Increasing the temperature by 63 °C increased the diffusion coefficient of the electroactive species in the ionic liquid electrolyte by a factor of approximately 5. The Walden product (the product of diffusion coefficient and the viscosity, $D \times \eta$) was constant over the temperature range studied ($3.1 \pm 0.06 \times 10^{-2}$ N cm), indicating that decreased viscosities at higher temperatures caused the observed increase in the diffusion coefficient. Comparison with the Arrhenius law (eq 1) allows the activation energy of diffusion to be calculated using linear plots of ln D versus T^{-1}.

$$D = D^{\theta} \exp\left(-\frac{\Delta H}{RT}\right) \quad (1)$$

Figure 4 shows plots of ln D versus T^{-1} for the reduced and oxidized forms of $[FcC_1MIm][NTf_2]$, which show good linearity over the range of temperatures studied. The activation energies for diffusion of $[FcC_1MIm]^+$ and $[FcC_1MIm]^{2+}$ were calculated to be 22.3 and 23.0 kJ mol^{-1}, respectively. These values are higher than those values determined for the diffusion of ferrocene in acetonitrile and DMF.[43] This is expected considering the reasonably high viscosity of the ionic liquid electrolyte used in this study compared to traditional organic solvents. As shown in Table 1, the ratio of the diffusion coefficients of the reduced and oxidized forms of $[FcC_1MIm]$ is greater than 1 at all temperatures studied. This behavior has been observed

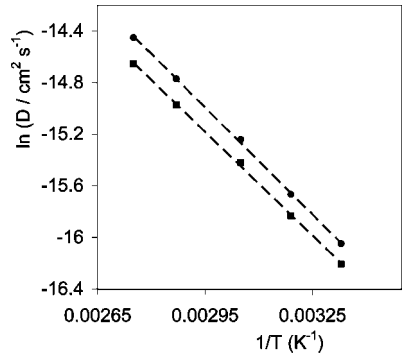

Figure 4. Plots of ln D versus T^{-1} for $[FcC_1MIm]^+$ (●) and $[FcC_1MIm]^{2+}$ (■).

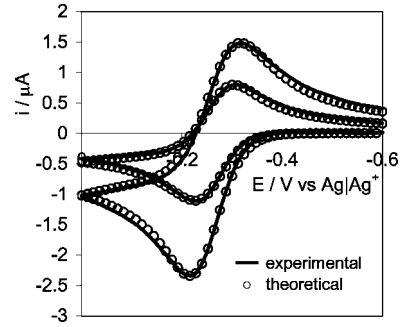

Figure 5. Experimental cyclic voltammograms obtained using 5 mM $[FcC_1MIm][NTf_2]$ in $[C_2MIm][NTf_2]$ at scan rates of (from top to bottom) 5 and 1 V s^{-1} (solid lines). The potential was scanned between −0.6 and 0.0 V vs $Ag|Ag^+$ and the working electrode was a nominally 0.25 mm radius platinum disk electrode. The initial potential was −0.6 V in each case. Simulated voltammograms generated according to the Butler−Volmer theory of electrode kinetics are shown by the open circles.

previously by others for various species dissolved in ionic liquid electrolytes and may be due to hindered diffusion of the oxidized species due to stronger solvation by the ionic liquid electrolyte.[45,46] It is also possible that ion pairing between the oxidized form of $[FcC_1MIm]$ and the RTIL contributes to the observed difference in diffusion coefficients.

Heterogeneous Electron Transfer Dynamics. As the scan rate in cyclic voltammetry is increased, the rate of heterogeneous electron transfer across the electrode/solution interface can influence the response causing an increase in ΔE_p. Figure 5 shows CVs obtained for 5 mM $[FcC_1MIm][NTf_2]$ in $[C_2MIm][NTf_2]$ at 1 and 5 V s^{-1}. At these scan rates, ΔE_p increased slightly with increasing scan rate. Because of the reasonably high specific conductivity of $[C_2MIm][NTf_2]$ (8.8 mS cm^{-1}) and the relatively small currents flowing at the electrode, the estimated ohmic drop is less than 1 mV, which is negligible compared to the observed ΔE_p. Therefore, the increased ΔE_p at these scan rates is most likely due to sluggish interfacial kinetics. Figure 5 also shows the theoretical responses simulated by integrating Fick's diffusion law and incorporating the Butler−Volmer theory of electrode kinetics. Excellent fits were obtained using values of $D = 1.08 \pm 0.07 \times 10^{-7}$ cm^2 s^{-1}, $\alpha = 0.4$ and $k^0 = 4.25 \pm 0.25 \times 10^{-3}$ cm s^{-1}. The value of k^0, determined using this approach, is similar to those reported by Compton[47] and Bond[48] for ferrocene in imidazolium RTILs. Given the drastically different solvent environment within an RTIL, the observation of a low k^0 in this system is not surprising. Moreover, considering the dependence of k^0 on solution viscosity, a small k^0 might be expected in an RTIL electrolyte.[49] However, this is based on the assumption that the effect of

solution viscosity on k^0 in this medium is similar to that observed in traditional solvents and a recent report has suggested this may not be true.[45] We are currently exploring the effect of RTIL viscosity and electrolyte composition on the heterogeneous electron transfer dynamics of this system. However, a description of these effects is beyond the scope of this paper and this will be described in a future contribution.

Scanning Electrochemical Microscopy. SECM has been extremely useful for probing the dynamics of heterogeneous electron transfer across the solid/liquid and liquid/liquid interface.[50,51] SECM has also been applied to kinetic studies at the interface between an ionic liquid and water.[31] However, the usefulness of SECM in single-phase ionic liquids has not been demonstrated clearly to date, and several authors have questioned the validity of conventional SECM theory in describing the behavior in ionic liquids.[33,34,52] However, no descriptions of SECM measurements in single-phase ionic liquids exist that employ both an electroactive ionic liquid analyte and an ionic liquid electrolyte, as is the case in this study. In developing this system, we were particularly interested in the effect of solubility on the SECM behavior of the RTIL analyte. In our measurements, the analyte was completely miscible with the RTIL electrolyte and, therefore, we completely eliminated any solubility issues from our system. This is in contrast with many other electrochemical investigations that employ RTIL electrolyte systems to investigate the electrochemistry of ferrocene. For example, the solubility of neutral ferrocene in $[C_2Mim][NTf_2]$ was examined by Compton and co-workers and found to be lower in this medium than in a range of other RTILs.[46]

In the case of finite heterogeneous kinetics at the tip and diffusion-controlled feedback at the substrate, the tip voltammogram may be described by eq 2:

$$i_T(E,L) = \frac{k_2}{L(\theta + 1/\kappa)} + \frac{k_1 + k_3 \exp(k_4/L)}{\theta\left[1 + \frac{\pi}{\kappa\theta}\frac{2\kappa\theta + 3\pi}{4\kappa\theta + 3\pi^2}\right]} \quad (2)$$

where k_1, k_2, k_3, and k_4 are constants, $i_T(E,L)$ is the tip current at potential E when positioned at a distance L from the substrate.[51] L is the normalized distance between the UME tip and the substrate, $L = d/a$, where d is the distance between the tip and the substrate and a is the radius of the tip. θ and κ are described below for an oxidation reaction:

$$\theta = 1 + \exp\left[\frac{F}{RT}(E - E^{0\prime})\right]\frac{D_O}{D_R} \quad (3)$$

$$\kappa = \pi\lambda \exp\left[\frac{(1-\alpha)F}{RT}(E - E^{0\prime})\right]/4I_T^C \quad (4)$$

where F is Faraday's constant, R is the gas constant, T is the temperature, $E^{0\prime}$ is the formal potential and D_O and D_R are the diffusion coefficients of the oxidized and reduced forms of the redox couple, respectively. The kinetic parameter, $\lambda = k^0 a/D$ and I_T^C is the normalized diffusion limiting tip current at distance L above a conductive substrate:

$$I_T^C = k_1 + k_2/L + k_3 \exp(k_4/L) \quad (5)$$

The tip used in these experiments had an RG value of approximately 2 based on optical microscopy. Therefore, the values of k_1, k_2, k_3, and k_4 are 0.6686604, 0.6973984, 0.3218171, and −1.744691, respectively.[32] The tip current described in eq 2 is normalized by the steady-state oxidation current at a disk ultramicroelectrode positioned far from any substrate electrode,

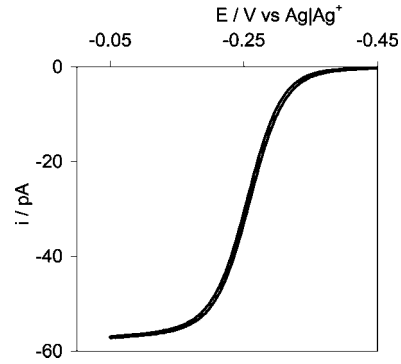

Figure 6. Steady-state voltammogram obtained at a 1.5 μm radius Pt SECM tip at a scan rate of 5 mV s^{-1}. The solution was 9 mM $[FcC_1Mim][NTf_2]$ in $[C_2MIm][NTf_2]$ and the potential was scanned between −0.45 and −0.05 V vs $Ag|Ag^+$. The initial potential was −0.45 V vs $Ag|Ag^+$.

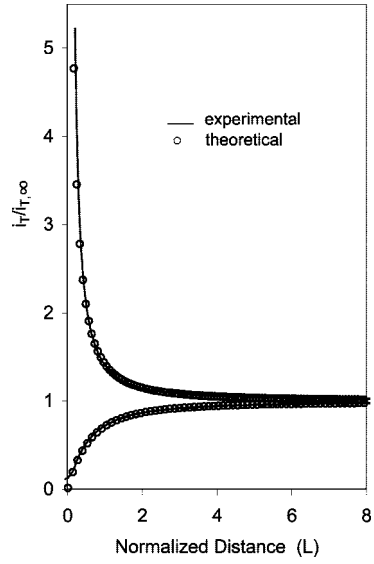

Figure 7. Negative (lower) and positive (upper) feedback approach curves obtained during the oxidation of $[FcC_1Mim][NTf_2]$ as the SECM tip approach a Teflon substrate and a 2 mm platinum disk substrate, respectively. In each case, the SECM tip was a 1.5 μm radius Pt UME, the solution was 9 mM $[FcC_1Mim][NTf_2]$ in $[C_2MIm][NTf_2]$ and the tip was held at 0.05 V vs $Ag|Ag^+$. The tip approach rate was 0.1 μm s^{-1} in each case. Experimental curves are shown by the solid lines and theoretical curves generated for a 1.5 μm tip with $RG = 2$ are shown by the open circles. During the positive feedback experiment, the substrate potential was held at −0.6 V vs $Ag|Ag^+$.

$i_{T,\infty}$, which is described in eq 6 for a disk ultramicroelectrode with $RG = 2$:[32]

$$i_{T,inf} = 4.43nFD_RCa \quad (6)$$

where C is the bulk solution concentration of the redox species. The constant 4.43 appears in eq 6 due to the small RG value of the electrode used here, which causes an increase in the availability of reactant diffusing from behind the plane of the electrode (i.e., a current increase of approximately 10% over that for an electrode with large RG).[53] The steady-state current obtained from slow scan rate (5 mV s^{-1}) CVs was 57 pA (Figure 6), which agrees closely with that predicted by eq 6 for a 1.5 μm radius platinum-disk SECM tip. Negative feedback approach curves were used to accurately determine the RG value as the shape of the negative feedback curve is highly dependent on the RG value. Figure 7 shows a positive and negative feedback approach curve obtained in a solution of $[FcC_1MIm][NTf_2]$ in

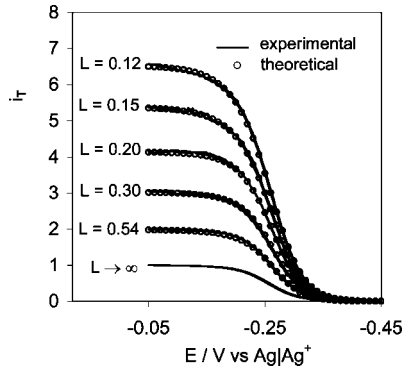

Figure 8. Experimental voltammograms (solid lines) obtained at a 1.5 μm radius platinum UME tip at distances of $L = 0.12$, 0.15, 0.20, 0.30, 0.54 and $L \rightarrow \infty$ from a 2 mm diameter platinum-disk substrate. The solution was 9 mM $[FcC_1Mim][NTf_2]$ in $[C_2MIm][NTf_2]$ and the substrate potential was held at -0.6 V vs $Ag|Ag^+$. The theoretical voltammograms at each distance (open circles) were calculated using eq 2.

$[C_2MIm][NTf_2]$ as the tip approached a platinum substrate and Teflon substrate, respectively. Also shown are the theoretical positive and negative feedback curves generated for a 1.5 μm radius SECM tip with $RG = 2$.[32,53] Clearly, excellent fits to the theoretical curves were obtained in each case, indicating that the radius and *RG* value of the SECM tip estimated using optical microscopy were accurate. Furthermore, the fits show that the radius determined from the steady-state CV shown in Figure 6 and eq 6 was accurate. The shape of the SECM curves was independent of the approach rate in the range studied (0.1−6 μm s^{-1}). However, slow approach rates were generally used in all cases to avoid accidentally crashing the tip into the substrate. In the negative feedback experiment, it was possible for the tip to approach the surface to a distance of approximately $L = 0.07$ ($I_T^C = 0.1$) before the insulating material crashed into the surface and caused a deviation from the theoretical negative feedback approach curve. Similarly, it was possible to approach the conducting surface to I_T^C values greater than 6 using these laser-pulled SECM tips. The fact that we were able to position the tip so close to the insulating and conducting substrates (which is crucial in kinetic measurements using the SECM) was due to careful sharpening (to reduce *RG*) and handling of the laser-pulled SECM tips.

In probing the heterogeneous electron transfer kinetics of oxidation of $[FcC_1MIm][NTf_2]$ at the SECM tip, the tip was held at various distances from a 2 mm diameter platinum disk substrate, and a tip voltammogram was recorded while holding the substrate at -0.6 V vs $Ag|Ag^+$. The *L* values used were 0.54, 0.30, 0.20, 0.15, and 0.12, which corresponded to distances, *d*, of approximately 810, 450, 300, 230, and 180 nm, respectively. The resulting i_T versus *E* curves were fitted to eq 2, and these are shown in Figure 8. The theoretical curves were generated using values of 1.07×10^{-7} and 0.914×10^{-7} cm^2 s^{-1} for the reduced and oxidized forms of $[FcC_1MIm][NTf_2]$, respectively (Table 1) and a tip radius of 1.5 μm. The solution concentration was 9 mM. The normalized i_T versus *E* curve obtained when the tip was positioned far from the substrate is also shown for comparison. Negligible hysteresis was detected in the CVs and high-quality fits were obtained at each *L* value. Table 2 shows the best-fit kinetic parameters for oxidation of $[FcC_1MIm][NTf_2]$ obtained from these voltammograms. The $E^{\circ\prime}$ values obtained from the best fits were stable to within 4 mV during the measurements, which is due to the high stability of the $Ag|Ag^+$ reference electrode in the RTIL electrolyte. The

TABLE 2: Kinetic Parameters for Oxidation of $[FcC_1MIm][NTf_2]$ at Pt SECM Tips at Various *L* Values[a]

L	10^3 k^0/cm s^{-1}	α	$E^{0\prime}$/V	λ'
∞	reversible			11 (λ)
0.53	6.9	0.51	−0.268	5.2
0.29	7.6	0.60	−0.270	3.1
0.20	7.9	0.64	−0.271	2.4
0.15	8.0	0.56	−0.271	1.6
0.12	7.7	0.61	−0.272	1.5

[a] $\lambda' = k^0 d/D$. λ at infinite distance was calculated using the average k^0 value and $\lambda = k^0 a/D$.

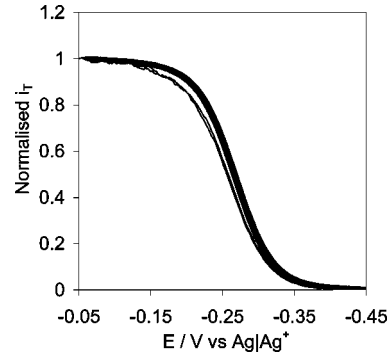

Figure 9. Normalized experimental SECM tip voltammograms obtained when the tip was located at a distance of $L = 0.12$ from the platinum substrate electrode (light line) and when the tip was located far from the substrate electrode (heavy line).

mean values of k^0 and α were $7.6 \pm 0.85 \times 10^{-3}$ cm s^{-1} and 0.56 ± 0.08 (95% confidence intervals). For a Nernstian response, the dimensionless parameter, $\lambda' = k^0 d/D = Lk^0 a/D \geq 10$,[51,54] that is, at small *L*, the rate of mass transfer to the tip increases and is a function of *d*. However, when the tip is far from the substrate, the condition of reversibility is $\lambda = k^0 a/D \geq 10$. Taking the mean value of k^0 from Table 2, $\lambda = 11$ when the tip was far from the substrate, indicating that the redox process was reversible. However, this value is very close to the limit for a truly Nernstian response, and it is possible that some slight deviation from an ideal reversible CV is present. Mirkin and Bard have calculated CVs at various *L* using different values of λ'.[55] They showed that, at $\lambda' = 10$, some small deviation of the curve from that with $\lambda' = 100$ is apparent and it is possible that the same effect is present in our measurements. Figure 9 shows the normalized voltammograms derived from the data shown in Figure 8 when the tip was positioned far from the substrate and when positioned at $L = 0.12$. Clearly, at this small value of *L*, the normalized voltammogram deviated from that observed when the tip was located far from the substrate in bulk solution. This observation confirms that, at small values of *d*, the rate of reaction at the SECM tip was governed by heterogeneous kinetics. The deviation of the CV obtained at small *L* from the CV obtained far from the substrate is relatively small and may be due to some quasi-reversibility of the CV response at large *L*. However, the uncertainty in the kinetic parameters shown in Table 2 is quite low (≈ 11%), indicating that the fits obtained at each *L* value yielded reliable kinetic data. Significantly, the value of k^0 determined using SECM is more than 50% larger than the value determined using cyclic voltammetry. Therefore, it is very likely that, even with careful fitting and background subtraction of the CVs, an underestimated k^0 was obtained in this medium using CV.

Using this RTIL analyte/electrolyte system, we have also obtained excellent steady-state responses at larger ultramicroelectrodes ($a = 5$ μm) as well as SECM feedback approach

curve data that agreed with theory at a range of approach rates using 5 μm tips. Therefore, it appears that the ability to perform such measurements using the SECM is not limited to using especially small tips or approach rates. It is possible that the very high solubility of the ionic liquid analyte in our system allows us to obtain these responses and perform such kinetic measurements using the SECM. In a following contribution, we will describe the effect of altering the counterion on the electrochemical behavior and will explore the effects of solution viscosity and composition on heterogeneous electron transfer kinetics in this medium using SECM. Thus, we anticipate that, by using SECM, we will be able obtain new insights into the role of the solvent during heterogeneous electron transfer reactions.

Conclusions

The electrochemical behavior of a ferrocene-based, redox-active ionic liquid, $[FcC_1MIm][NTf_2]$, in an ionic liquid electrolyte, $[C_2MIm][NTf_2]$, has been examined using cyclic voltammetry and SECM. Remarkably ideal responses were obtained for the ferrocene moiety in acetonitrile and in the ionic liquid electrolyte. Because of the relatively high viscosity of the ionic liquid electrolyte, the diffusion coefficient of $[FcC_1MIm][NTf_2]$ was 2 orders of magnitude smaller than when dissolved in acetonitrile. Variable-temperature voltammetry showed a significant increase in the rate of diffusion of the redox-active species with a moderate increase in the temperature. The standard rate constant for heterogeneous electron transfer across the electrode/ionic liquid interface was determined to be 4.25×10^{-3} cm s^{-1} using cyclic voltammetry. SECM was also used to probe the kinetics of heterogeneous electron transfer across the electrode/ionic liquid interface. Despite the low diffusion coefficient of the redox-active species, excellent steady-state cyclic voltammograms were obtained at the SECM tip, and the SECM responses agreed with those predicted using conventional SECM theory. Thus, we have shown here for the first time that SECM is a very useful technique for measuring heterogeneous electron transfer kinetics at the metal/ionic liquid interface. Furthermore, it appears that SECM can provide more reliable kinetic data than cyclic voltammetry, which may lead to underestimated values of k^0. It is possible that the ideal responses observed using the present system are due to the high solubility of the ionic liquid analyte in the ionic liquid electrolyte, and this will be explored further in a future contribution.

Acknowledgment. We thank the UK Engineering and Physical Sciences Research Council (EPSRC) for funding through the DICE (Driving Innovation in Chemistry and Chemical Engineering) Project under the Science and Innovation Award (Grant Number EP/D501229/1). P.L. is currently holder of an EPSRC Advanced Research Fellowship (EP/D073014/1).

References and Notes

(1) Borra, E. F.; Seddiki, O.; Angel, R.; Eisenstein, D.; Hickson, P.; Seddon, K. R.; Worden, S. P. *Nature* **2007**, *447*, 979.
(2) Rogers, R. D.; Seddon, K. R. *Science* **2003**, *302*, 792.
(3) Zhao, H.; Holladay, J. E.; Brown, H.; Zhang, Z. C. *Science* **2007**, *316*, 1597.
(4) *Ionic Liquids in Synthesis*; Wasserscheid, P., Welton, T., Eds.; Wiley-VCH: Weinheim, 2003.
(5) Miao, W.; Chan, T. H. *Acc. Chem. Res.* **2006**, *39*, 897.
(6) Jiang, Y.; Xia, H.; Guo, C.; Mahmood, I.; Liu, H. *Ind. Eng. Chem. Res.* **2007**, *46*, 6303.
(7) Huang, C.; Chen, B.; Zhang, J.; Liu, Z.; Li, Y. *Energy Fuels* **2004**, *18*, 1862.
(8) Erbeldinger, M.; Mesiano, A. J.; Russell, A. J. *Biotechnol. Prog.* **2000**, *16*, 1129.
(9) Gubicza, L.; Nemestóthy, N.; Fráter, T.; Bélafi-Bakó, K. *Green Chem.* **2003**, *2*, 236.
(10) Frackowiak, E.; Lota, G.; Pernak, J. *Appl. Phys. Lett.* **2005**, *86*, 164104.
(11) Balducci, A.; Dugas, R.; Taberna, P. L.; Simon, P.; Plée, D.; Mastragostino, M.; Passerini, S. *J. Power Sources* **2007**, *165*, 922.
(12) Bansal, D.; Cassel, F.; Croce, F.; Hendrickson, M.; Plichta, E.; Salomon, M. *J. Phys. Chem. B* **2005**, *109*, 4492.
(13) Lee, S.-Y.; Yong, H. H.; Lee, Y. J.; Kim, S. K.; Ahn, S. *J. Phys. Chem. B* **2005**, *109*, 13663.
(14) Fredin, K.; Gorlov, M.; Pettersson, H.; Hagfeldt, A.; Kloo, L.; Boschloo, G. *J. Phys. Chem. C* **2007**, *111*, 13261.
(15) Pinilla, C.; Del Popolo, M. G.; Lynden-Bell, R. M.; Kohanoff, J. *J. Phys. Chem. B* **2005**, *109*, 17922.
(16) Tsuda, T.; Hussey, C. L.; Stafford, G. R. Bonevich, J. E. *J. Electrochem. Soc.* **2003**, *150*, C234.
(17) El Abedin, S. Z.; Pölleth, M.; Meiss, S. A.; Janek, J.; Endres, F. *Green Chem.* **2007**, *6*, 549.
(18) Wilkes, J. S.; Zaworotko, M. J. *J. Chem. Soc., Chem. Commun.* **1992**, 965.
(19) Bonhote, P.; Dias, A.-P.; Papageorgiou, N.; Kalyanasundaram, K.; Gratzel, M. *Inorg. Chem.* **1996**, *35*, 1168.
(20) Matsumiya, M.; Terazono, M.; Tokuraku, K. *Electrochim. Acta* **2006**, *51*, 1178.
(21) Lagrost, C.; Preda, L.; Volanschi, E.; Hapiot, P. *J. Electroanal. Chem.* **2005**, *585*, 1.
(22) Schroder, U.; Wadhawan, J. D.; Compton, R. G.; Marken, F.; Suarez, P. A. Z.; Consorti, C. S.; De Souza, R. F.; Dupont, J. *New J. Chem.* **2000**, *24*, 1009.
(23) Zhang, J.; Bond, A. M. *Analyst* **2005**, *130*, 1132.
(24) Hultgren, V. M.; Mariotti, A. W. A.; Bond, A. M.; Wedd, A. G. *Anal. Chem.* **2002**, *74*, 3151.
(25) Bond, A. M.; Oldham, K. B.; Snook, G. A. *Anal. Chem.* **2000**, *72*, 3492.
(26) Fitchett, B. D.; Knepp, T. N.; Conboy, J. C. *J. Electrochem. Soc.* **2004**, *151*, E219.
(27) Buzzeo, M. C.; Hardacre, C.; Compton, R. G. *ChemPhysChem* **2006**, *7*, 176.
(28) Holbrey, J. D.; Reichert, W. M.; Swatloski, R. P.; Broker, G. A.; Pitner, W. P.; Seddon, K. R.; Rogers, R. D. *Green Chem.* **2002**, *4*, 407.
(29) Zhao, F.; Wu, X.; Wang, M.; Liu, Y.; Gao, L.; Dong, S. *Anal. Chem.* **2004**, *76*, 4960.
(30) Laforge, F. O.; Kakiuchi, T.; Shigematsu, F.; Mirkin, M. V. *Langmuir* **2006**, *22*, 10705.
(31) Laforge, F. O.; Kakiuchi, T.; Shigematsu, F.; Mirkin, M. V. *J. Am. Chem. Soc.* **2004**, *126*, 15380.
(32) Mirkin, M. V. In *Scanning Electrochemical Microscopy*; Bard, A. J., Mirkin, M. V., Eds.; Marcel Dekker: New York, 2001; pp 145−198.
(33) Carano, M.; Bond, A. M. *Aust. J. Chem.* **2007**, *60*, 29.
(34) Ghilane, J.; Lagrost, C.; Hapiot, P. *Anal. Chem.* **2007**, *79*, 7383.
(35) Gao, Y.; Twanley, B.; Shreeve, J. M. *Inorg. Chem.* **2004**, *43*, 3406.
(36) Bolm, C.; Kesselgruber, M.; Raabe, G. *Organometallics* **2002**, *21*, 707.
(37) Thomas, J.-L.; Howarth, J.; Hanlon, K.; McGuirk, D. *Tetrahedron Lett.* **2000**, *41*, 413.
(38) Balasubramanian, R.; Wang, W.; Murray, R. W. *J. Am. Chem. Soc.* **2006**, *128*, 9994.
(39) Snook, G. A.; Best, A. S.; Pandolfo, A. G.; Hollenkamp, A. F. *Electrochem. Commun.* **2006**, *8*, 1405.
(40) Mauzeroll, J.; LeSuer, R. J. In *Handbook of Electrochemistry*; Zoski, C. G., Ed.; Elsevier B. V.: The Netherlands, 2007; pp 199−211.
(41) Bard, A. J.; Faulkner, L. R. *Electrochemical Methods: Fundamentals and Applications*, 2nd Ed. ; Wiley: New York, 2001.
(42) Kamau, G. N.; Saccucci, T. M.; Gounili, G.; Nassar, A.-E. F.; Rusling, J. F. *Anal. Chem.* **1994**, *66*, 994.
(43) Jacob, S. R.; Hong, Q.; Coles, B. A.; Compton, R. G. *J. Phys. Chem. B* **1999**, *103*, 2963.
(44) Kosmulski, M.; Osteryoung, R. A.; Ciszkowskab, M. *J. Electrochem. Soc.* **2000**, *147*, 1454.
(45) Belding, S. R.; Rees, N. V.; Aldous, L.; Hardacre, C.; Compton, R. G. *J. Phys. Chem. C* **2008**, *112*, 1650.
(46) Rogers, E.; Silvester, D. S.; Poole, D. L.; Aldous, L.; Hardacre, C.; Compton, R. G. *J. Phys. Chem. C* **2008**, *112*, 2729.
(47) Barnes, A. S.; Rogers, E. I.; Streeter, I.; Aldous, L.; Hardacre, C.; Compton, R. G. *J. Phys. Chem. B* **2008**, *112*, 7560.
(48) Zhang, J.; Bond, A. M. *Anal. Chem.* **2003**, *75*, 2694.
(49) Zhang, X.; Leddy, J.; Bard, A. J. *J. Am. Chem. Soc.* **1985**, *107*, 3719.

(50) Borgwarth, K.; Heinze, J. In *Scanning Electrochemical Microscopy*; Bard, A. J., Mirkin, M. V., Eds.; Marcel Dekker: New York, 2001; pp 201−238.
(51) Sun, P.; Mirkin, M. V. *Anal. Chem.* **2006**, *78*, 6526.
(52) Nkuku, C. A.; LeSuer, R. J. *J. Phys. Chem. B* **2007**, *111*, 13271.
(53) Amphlett, J. L.; Denault, G. *J. Phys. Chem. B* **1998**, *102*, 9946.
(54) Mirkin, M. V.; Bard, A. J. *Anal. Chem.* **1992**, *64*, 2293.
(55) Mirkin, M. V.; Richards, T. C.; Bard, A. J. *J. Phys. Chem.* **1993**, *97*, 7672.

JP8024717